HHS Public Access

Author manuscript

J Am Coll Cardiol. Author manuscript; available in PMC 2017 March 08.

Published in final edited form as:

J Am Coll Cardiol. 2016 March 8; 67(9): 1074–1086. doi:10.1016/j.jacc.2015.12.035.

Evidence for Mechanisms Underlying the Functional Benefits of a Myocardial Matrix Hydrogel for Post-MI Treatment

Jean W. Wassenaar, BS[a,b], **Roberto Gaetani, PhD**[a,b], **Julian J. Garcia**[a,b], **Rebecca L. Braden, MS**[a,b], **Colin G. Luo, MS**[c], **Diane Huang, BS**[c], **Anthony N. DeMaria, MD**[c], **Jeffrey H. Omens, PhD**[a,c], and **Karen L. Christman, PhD**[a,b]

[a]Department of Bioengineering, University of California, San Diego, La Jolla, California

[b]Sanford Consortium for Regenerative Medicine, La Jolla, California

[c]Department of Medicine, University of California, San Diego, La Jolla, California

Abstract

BACKGROUND—There is increasing need for better therapies to prevent the development of heart failure after myocardial infarction (MI). An injectable hydrogel derived from decellularized porcine ventricular myocardium has been shown to halt the post-infarction progression of negative left ventricular remodeling and decline in cardiac function in both small and large animal models.

OBJECTIVES—We sought to elucidate the tissue level mechanisms underlying the therapeutic benefits of myocardial matrix injection.

METHODS—Myocardial matrix or saline was injected into infarcted myocardium 1 week after ischemia-reperfusion in Sprague Dawley rats. Cardiac function was evaluated by magnetic resonance imaging and hemodynamic measurements at 5 weeks post-injection. Whole transcriptome microarrays were performed on ribonucleic acid (RNA) isolated from the infarct at 3 days and 1 week after injection. Quantitative polymerase chain reaction and histological quantification confirmed expression of key genes and their activation in altered pathways.

RESULTS—Principal component analysis of the transcriptomes showed that samples collected from myocardial matrix-injected infarcts are distinct and cluster separately from saline-injected controls. Pathway analysis indicated that these differences are due to changes in several tissue processes that may contribute to improved cardiac healing post-MI. Matrix-injected infarcted myocardium exhibits an altered inflammatory response, reduced cardiomyocyte apoptosis, enhanced infarct neovascularization, diminished cardiac hypertrophy and fibrosis, altered metabolic enzyme expression, increased cardiac transcription factor expression, and progenitor cell recruitment, along with improvements in global cardiac function and hemodynamics.

Address for correspondence: Karen L. Christman, PhD, 2880 Torrey Pines Scenic Drive, La Jolla, California 92037, Telephone: (858) 822-7863, Fax: (858) 534-5722, christman@eng.ucsd.edu.

Disclosures: The other authors have nothing to disclose

CONCLUSIONS—These results indicate that the myocardial matrix alters several key pathways post-MI creating a pro-regenerative environment, further demonstrating its promise as a potential post-MI therapy.

Keywords

biomaterial; extracellular matrix; heart failure; microarray; infarction

Progression from acute myocardial infarction (MI) to chronic heart failure (HF) begins with an initial ischemic injury, resulting in progressive myocyte loss through both necrotic and apoptotic mechanisms, and migration of inflammatory cells into the injured myocardium. An increase in matrix metalloproteinases (MMP) from the inflammatory infiltrate further exacerbates the decline in heart function by digesting the extracellular matrix (ECM), followed by subsequent deposition of fibrillar cross-linked collagen. The heart has recently been recognized as an organ capable of some degree of self-regeneration (1). However, this is insufficient to compensate for the billions of cardiomyocytes lost after MI (2). Additionally, function of surviving cardiomyocytes is also altered post-infarction. The heart has a high energy demand and recent studies have shown that dysregulation in cardiac metabolism post-MI contributes notably to cardiac dysfunction in HF (3).

Interest in developing alternative treatments for MI has been expanding. Such therapies include various cells, biological molecules, acellular biomaterials, or combinations thereof. Meta-analyses of initial cell therapy trials suggest only a modest effect on cardiac function (4), and given low cell survival rates and their largely paracrine mechanism of action, there has been increasing interest in the use of injectable acellular scaffolds (5). If designed appropriately, these biomaterials can be delivered through minimally invasive approaches and stimulate cardiac repair, while avoiding many of the complications associated with a living product (6). Our group previously developed an injectable myocardial matrix hydrogel, derived from decellularized porcine ventricular ECM (7), which can be delivered with a transendocardial catheter. This hydrogel was shown to reduce negative left ventricular (LV) remodeling and the decline in cardiac function in both rat (8) and pig (9) models when delivered 2 weeks post-MI. Herein, we examined whether the material could improve global cardiac function and hemodynamics when delivered 1 week post-MI in a rat model, and utilized a transcriptomics-directed approach to identify the underlying mechanisms by which the matrix improves post-MI repair.

METHODS

All procedures in this study were approved by the Committee on Animal Research at the University of California, San Diego and the Association for the Assessment and Accreditation of Laboratory Animal Care. Myocardial matrix or saline was injected into the area of ischemia 1 week after 25 minutes of ischemia-reperfusion in female Sprague-Dawley rats. Rat Gene 2.0 ST arrays (Affymetrix, Inc., Santa Clara, California) were used for whole transcriptome analysis of infarct and border zone at 3 days and 1 week post-injection, followed by validation of the expression of key genes by quantitative real-time polymerase chain reaction (qPCR). Cardiac magnetic resonance imaging (CMR) and hemodynamics

recordings were performed at 5 weeks post-injection (6 weeks post-MI). Histology and immunohistochemistry (IHC) were used to quantify phenotypic changes. For further details, refer to the Online Appendix.

RESULTS

CARDIAC FUNCTION

Myocardial matrix injection (n = 8) significantly reduced the percent change in ejection fraction (p = 0.028) and end-systolic volume (p = 0.004) compared to saline (n = 7) (Figure 1A) from 6 days post-MI (1 day prior to injection) to 6 weeks post-MI (5 weeks post-injection). There was a similar but nonsignificant trend for end-diastolic volume (p = 0.11). CMR data are provided in Online Table 1. LV hemodynamics were measured using a microtipped manometer pressure catheter at 6 weeks post-MI (Figure 1B). Compared to saline (n = 5), myocardial matrix-injected hearts (n = 5) had significantly higher LV peak systolic pressure (p = 0.002), myocardial relaxation ($-dP/dt_{max}$; p = 0.003), and myocardial contractility ($+dP/dt_{max}$; p = 0.002).

TRANSCRIPTOMICS

Differences in transcriptomes between saline- and matrix-treated infarcts were globally examined using both principal component analysis (PCA) and hierarchical clustering. Saline- and myocardial matrix-injected samples did not cluster separately at 3 days post-injection. However, by 1 week post-injection, both PCA (Figure 2A) and hierarchical clustering (Figures 2B and 2C) showed separation of the transcriptomes (p = 0.06), indicating a shift in global gene expression. A false discovery rate of $q < 0.05$ was used to determine the differentially expressed genes for biological interpretation (Online Table 2). A Panther overrepresentation test showed that differences in transcripts from ECM (GO: 0031012 by Gene Ontology [GO]) and those responsible for muscle contraction (GO: 006936) for the 1-week time point were nonsignificant (p = 0.37 and p = 0.88, respectively), indicating that differences in gene expression were not due to sampling variability. Using Ingenuity® Pathway Analysis (IPA) (Qiagen, Redwood City, California), we identified the main effects of the myocardial matrix at 3 days post-injection as downregulation of apoptosis, upregulation of blood vessel development, and increase in cell movement (Online Table 3). By 1 week, several pathways were significantly activated, including downregulation of cell death and hypertrophy, and upregulation of many metabolic processes and gene translation/transcription (Online Table 4). Based on the differences elucidated by this transcriptome analysis, we performed qPCR on key genes in the identified pathways (Online Figure 1) and further assessed differences at the tissue level using IHC as described later.

INFLAMMATORY RESPONSE

Pathways involved in the immune response including migration and infiltration of various cell types were predicted at both the 3-day and 1-week time points (Online Tables 3 and 4, Figure 3A, and Online Figure 2). Similarly, a substantial number of genes at both time points – 26.6% at day 3 and 9.8% at 1 week – were characterized as part of immune response process (GO:0002376). Increased expression of CD68 (p = 0.045) and MMP12 (p

= 0.043) (Online Figure 1A) were confirmed by qPCR, indicative of increased macrophage infiltration as a result of matrix injection, yet IHC analysis using a CD68 antibody (Figure 3B) did not show a difference in macrophage infiltration between saline- and matrix-injected infarcts at 3 days (Figure 3C). There was, however, a trend towards an increase in infiltrating tryptase+ mast cells (Figure 3D) at 3 days (p = 0.052), which reached significance by 1 week (p = 0.032) (Figure 3E).

BLOOD VESSEL FORMATION

Activation of blood vessel development was predicted by IPA at 3 days post-injection (Online Table 3 and Figure 4A). While increased vessel development was not directly predicted at 1 week post-injection, many growth factors associated with angiogenesis and neovascularization were identified (Figure 4A). These included a decrease in angiopoietin-2 (p = 0.012) and increases in acidic fibroblast growth factor (p = 0.053) and vascular endothelial growth factors A and B (p = 0.034 and p = 0.009 respectively), confirmed by qPCR (Online Figure 1B). Infarct vascularization was then examined by IHC (Figure 4B). While not significantly different at 3 days post-injection, capillary density was significantly higher in the matrix-injected group at 1 week (p = 0.038) (Figure 4C). Arteriole density showed a similar result, with no difference at 3 days, but a trend towards an increase at 1 week in the matrix group (p = 0.056) (Figure 4D). When subdivided into large (Online Figure 3A), medium (Online Figure 3B), and small (Online Figure 3C) arterioles, there was a trend at 3 days for increased small arterioles within matrix-injected infarcts (p = 0.082), which shifted at 1 week to a significant increase in medium (p = 0.021) and a trend for an increase in large diameter vessels (p = 0.065).

CARDIOMYOCYTE APOPTOSIS

Decreased apoptosis was consistently predicted by IPA at both 3 days and 1 week post-injection (Online Tables 3 and 4, Figure 5A, and Online Figures 4 and 5). Increased expression of antioxidative enzymes heme oxygenase 1 (p = 0.015) at 3 days and catalase (p = 0.002) at 1 week, as well as the antiapoptosis regulator Bcl-2 (p = 0.006) at 1 week, were confirmed using qPCR (Online Figure 1C). To determine the effect myocardial matrix injection may have on apoptosis of cardiomyocytes specifically, anti-cleaved-Caspase3 staining with colabeling of cardiomyocytes using α-actinin was performed (Figure 5B). Quantification of the number of caspase-3-expressing cardiomyocytes within the infarct wall showed a trend towards decreased apoptotic cardiomyocytes within the infarct wall (p = 0.085) at 3 days post-injection (Figure 5C).

CARDIAC METABOLISM

At 1 week post-injection, several genes associated with oxidative metabolism and mitochondrial biogenesis were upregulated and predicted to be activated by IPA (Online Table 4, Figure 6A, and Online Figures 6 and 7). Similarly, GO analysis classified 53% of the differentially expressed transcripts to be involved in metabolic processes (GO:008152). Within these genes, we identified several upregulated nuclear receptors involved in cardiac metabolism and mitochondrial biogenesis, including increased expression of the transcription co-activator peroxisome proliferator-activated receptor (PPAR) gamma coactivator 1-alpha (PGC-1α) (p = 0.006) and several of its target receptors, including

estrogen-related receptor (ERR) γ (p = 0.001) and PPARα (p = 0.032) and β/δ (p = 0.018), which were confirmed by qPCR (Online Figure 1D). To determine whether changes in metabolism were specifically associated with cardiomyocytes, IHC was performed to identify expression of PGC-1α within cardiomyocytes (Figure 6B). Quantification of PGC-1α+ cardiomyocytes adjacent to the infarct scar revealed that myocardial matrix-injected hearts exhibited a higher percentage of PGC-1α expression compared to saline-injected hearts (p = 0.009) (Figure 6C).

CARDIAC DEVELOPMENT AND PROGENITORS

Review of significant GO terms showed several associated with muscle development, including heart development (GO:0007507; Figure 7A), and qPCR-confirmed consistent elevated expression of GATA4 (p = 0.022), Nkx2.5 (p = 0.009), MEF2d (p = 0.004), myocardin (p = 0.004), Tbx5 (p = 0.012), and Tbx20 (p = 0.043) (Online Figure 1E). We also assessed infiltration of cells expressing cKit, a commonly used marker for cardiac progenitor cells (CPCs). Since cKit is also expressed by mast cells, tissue sections were costained with antimast cell tryptase (Figure 7B). Quantification of cKit+/tryptase-cells in the infarct wall showed a trend at 3 days (p = 0.067), which reached significance at 1 week (p = 0.031) in the matrix-injected group (Figure 7C). Costaining showed some of these cells expressed the cardiac transcription factor Nkx2.5 (Online Figure 8).

HYPERTROPHY AND FIBROSIS

At 1 week post-injection, cardiac hypertrophy was highly represented in the pathways predicted to be downregulated by IPA (Online Table 4, Figure 8A, and Online Figure 9). Increased expression of negative regulators of hypertrophy DUSP5 (p = 0.003) and DYRK1a (p = 0.004) as well as a decrease in the positive regulator NUPR1 (p = 0.048) were all confirmed by qPCR (Online Figure 1F). The effects on hypertrophic LV remodeling were therefore assessed at 5 weeks post-injection by measuring cardiomyocyte diameter to evaluate cardiomyocyte hypertrophy (Figure 8B) and staining with Mason's trichrome to evaluate interstitial fibrosis in the remote myocardium. Quantification of cross-sectional areas showed a trend in the matrix-injected hearts (n = 7) toward less hypertrophic cardiomyocytes (p = 0.061) (Figure 8C) compared to saline (n = 8). Moreover, myocardial matrix injection was associated with significantly reduced interstitial fibrosis (p < 0.001) (Figure 8D).

DISCUSSION

Previous small and large animal studies have demonstrated that injection of acellular myocardial matrix improved cardiac function and reduced negative LV remodeling when delivered 2 weeks post-MI. Importantly, biocompatibility, hemocompatibility, and lack of arrhythmias were demonstrated (8,9). In the current study, we analyzed infarct gene expression using wholetranscriptome microarrays to gain a comprehensive understanding of the tissue-level mechanism of action of the myocardial matrix hydrogel. Gene expression was analyzed at both 3 days and 1 week post-injection based on previous studies indicating that cellular infiltration into the injected hydrogel was most pronounced during the first week (9). By 1 week post-injection, the transcriptomes of saline and matrix-injected infarcts

clustered separately. Similar analyses have also been applied to other experimental therapies for MI including cell transplantation (10–12) and injection of cell-derived products (13); however, to our knowledge, no other biologic-based therapy has been reported to induce a distinct transcription signature at a global level. In this study, the key modulated pathways included inflammation, reduction of apoptosis and cardiac hypertrophy, metabolism, and blood vessel and cardiac development (Central Illustration).

Gene expression differences within the infarct suggested an increase in macrophage migration in response to the matrix injection with increased transcription of CD68, a macrophage marker, and MMP12, a macrophage-specific protease (14). However, differences in transcription patterns could also be attributed to changes in immune cell behavior since an increase in macrophages was not demonstrated. Collective analysis of all differentially expressed transcripts related to inflammation was not conclusive regarding whether there was a predominance of either M1 or M2 macrophage activation, which has been attributed to pro-inflammatory and proremodeling responses, respectively (15). Both phenotypes are likely necessary for post-infarct repair as depletion of either M1 or M2 macrophages inhibited the ability of neonatal hearts to regenerate post-MI (16). In the process of identifying c-Kit+ progenitors, which stain negative for tryptase, we detected a notable increase in the number of tryptase+ mast cells in the matrix-injected groups. While mast cells are traditionally associated with an allergic response, they are also involved in neovascularization and regulation of the immune response (17). Following ischemia, rapid mast cell degranulation occurs, triggering recruitment of other leukocytes and preventing cardiomyocyte apoptosis (18). Additionally, mast cell products are known to be inherently angiogenic and stimulate endothelial secretion of angiogenic chemokines (19). While it is known that mast cell activation may be the first step in the acute inflammatory response to implanted biomaterials (20), implication on the reparative response of decellularized materials has not been reported.

By 1 week post-injection, myocardial matrix had also significantly increased infarct neovasculature. Interestingly, the changes over time appeared to be due to a decrease in endothelial cells and arterioles in the saline-injected controls. Immediately post-MI, hypoxia-inducible factor expression triggers transcriptional activation of many angiogenic factors (21); however, a decrease in vascular density with time has been previously reported (22), possibly due to vessel regression. Notably, 1 factor known to induce this process is angiopoietin 2, which was more highly expressed in the saline group compared to the matrix. Preservation of the infarct vasculature may be a result of the pro-angiogenic milieu induced by the myocardial matrix, whether indirectly, through its effects on other cell types such as immune cells, or directly, by creating a new physical scaffold for vessel infiltration or releasing bioactive matricryptic peptides from partial proteolysis of the ECM (23).

Pathway analysis from the microarray data predicted consistent downregulation of apoptosis and cell death. Specifically, matrix-injected infarcts expressed higher levels of heme oxygenase 1 at 3 days and catalase at 1 week, both of which are stress-induced enzymes that reduce reactive oxygen species. In the histological analysis, we demonstrated a trend towards a reduction in cardiomyocyte apoptosis in the infarct wall. After an infarct, cardiomyocyte death peaks 24 hours after the injury then decreases, but continues to be

elevated above baseline levels for at least 12 weeks (24). Therefore, delivery of the myocardial matrix could play an important role in salvaging cardiomyocytes that are pre-apoptotic. Pathway analysis also predicted upregulation of genes involved in mitochondrial metabolism. It is well demonstrated that myocardial ischemia reduces substrate oxidation, resulting in an increased reliance on glycolysis (25). After matrix injection, we found increased expression of PGC-1α, PPARα, PPARβ/δ, and ERRγ. The PGC-1α activates the transcription of these nuclear receptors to increase fatty acid uptake, oxidative phosphorylation, and mitochondrial biogenesis (26). Expression of PGC-1α targets is known to be downregulated in both rodent models and patients with HF (27). We showed an increase in PGC-1α in cardiomyocytes in matrix-injected animals. In comparison, injections of various bone marrow cells into the infarct myocardium have been associated with decreased expression of genes related to mitochondrial function (10,12). Angiotensin-converting enzyme inhibition using captopril, a common treatment for HF, similarly did not rescue changes in fatty acid metabolism (28).

The adult mammalian heart has a limited ability to regenerate, and many recent efforts have attempted to enhance this ability post-MI (2). GO analysis suggested activation of terms related to heart and cardiovascular system development, which led us to investigate whether there was an upregulation of cardiac transcription factors known to play a role in cardiac regeneration. We found increased expression of 6 cardiac transcription factors. Of these, GATA4, myocardin, Nkx2.5, Tbx5, and Tbx20 are all expressed throughout various stages of embryonic cardiogenesis (29), while GATA4, Nkx2.5, and Tbx5 are frequently used to identify various CPC subsets (30). Increased expression of MEF and GATA4 were reported following injection of bone marrow cells and mononuclear cell secretomes (10,13); however, to our knowledge, concomitant elevated transcription of several cardiac transcription factors has not been previously reported. A lineage tracing study will however be necessary to determine whether the myocardial matrix can induce cardiac regeneration, as elevated expressions of these factors can occur during other processes. For example, GATA4, myocardin, Nkx2.5, and Tbx20 are expressed by adult cardiomyocytes and are required for their survival and function (31–34); cardiac hypertrophy is associated with elevated GATA4, MEF2d, and Nkx2.5 (35,36); and cardiac fibroblasts can express high levels of GATA4 and Tbx20 (37). We, however, show an increase of 6 transcription factors for cardiac development, along with a decrease in cardiac hypertrophy and fibrosis. We also found a significant increase in ckit+/tryptase-CPCs in matrix-injected hearts. Previously, the myocardial matrix was shown to promote cardiac differentiation of cKit+ CPCs in vitro (38). In this study, we found some cKit+ cells coexpressing Nkx2.5, which has been used to identify cardiac lineage differentiation in vivo (39). The importance of ckit+ cells in post-infarct regeneration, however, has been a controversial subject and 2 recent studies arrived at opposite conclusions (40,41). Additionally, cKit+ cells may contribute to other effects of the myocardial matrix injection, such as neovascularization (41).

Previous studies with myocardial matrix tested delivery at 2 weeks post-MI (8,9). In the current study we injected the material 1 week post-MI, demonstrating that the matrix can also be effective at an earlier time point. Hemodynamics, which had not been previously studied, further demonstrated improvements in LV peak systolic pressure, myocardial contractility, and myocardial relaxation. As further evidence that the matrix attenuates

negative LV remodeling, decreased hypertrophy was suggested by transcriptional analysis as early as 1 week postinjection, and there was a trend towards a reduction in cardiomyocyte area and a significant reduction in interstitial fibrosis by 5 weeks.

STUDY LIMITATIONS

Limitations of this study include the use of a small animal model, relatively short time points of assessment post-injection, and the more mild ischemia-reperfusion model, which is likely more representative of the acute or sub-acute MI population rather than severe remodeling in HF patients. While changes in cardiac function were significant in this and a previous rat MI study, with similar injections and time points (8), larger increases in function were observed in a large animal model where the infarct was more severe, multiple injections were performed across the infarct, and cardiac function was examined out to 3 months post-injection (9). Unlike cells or growth factors, which have had diminished efficacy in moving from small to large animals, biomaterials may have the capacity for greater improvements in larger animals (42), which is promising for future clinical translation. This study also tested a porcine-derived ECM hydrogel in a rat model, which has potential for xenograft-elicited inflammation. However, we observed similar improvements in a porcine MI model with the porcine-derived material (9), suggesting that the interspecies effects are not a major factor. Also, this study mimicked the xenogeneic porcine material source being used in an ongoing clinical trial (Clinicaltrials.gov identifier NCT02305602).

CONCLUSIONS

In this study, we demonstrated reduced negative LV remodeling and improved hemodynamics following delivery of myocardial matrix 1 week post-MI. We provided both transcriptional and histological evidence that the myocardial matrix mediated this by inducing various tissue level changes. These results provide further evidence for the promise of the myocardial matrix as a therapy to prevent development of HF post-MI.

Supplementary Material

Refer to Web version on PubMed Central for supplementary material.

Acknowledgments

This research was funded in part by the NIH NHLBI (1R01HL113468). JWW was supported by pre-doctoral fellowships from the California Institute for Regenerative Medicine and the American Heart Association, as well as the University of California, San Diego Medical Scientist Training Program T32 GM007198-40. AND is a scientific advisory board member, and KLC is a co-founder, board member, consultant, and holds equity interest in Ventrix, Inc.

The authors would like to thank Dr. Nicholas Webster of the San Diego VA/VAMF Microarray and NGS Core for assistance with microarray analysis as well as Dr. Christian Metallo for helpful discussions regarding metabolism. This research was funded in part by the NIH NHLBI (1R01HL113468). JWW was supported by pre-doctoral fellowships from the California Institute for Regenerative Medicine and the American Heart Association, as well as the University of California, San Diego Medical Scientist Training Program T32 GM007198-40. AND is a scientific advisory board member, and KLC is a co-founder, board member, consultant, and holds equity interest in Ventrix, Inc.

ABBREVIATIONS AND ACRONYMS

CPC	cardiac progenitor cell
ECM	extracellular matrix
EDV	end-diastolic volume
IHC	immunohistochemistry
LV	left ventricle
MI	myocardial infarction
qPCR	quantitative real-time polymerase chain reaction

REFERENCES

1. Leri A, Kajstura J, Anversa P. Role of Cardiac Stem Cells in Cardiac Pathophysiology: A Paradigm Shift in Human Myocardial Biology. Circ Res. 2011; 109:941–961. [PubMed: 21960726]
2. Xin M, Olson EN, Bassel-Duby R. Mending broken hearts: cardiac development as a basis for adult heart regeneration and repair. Nat Rev Mol Cell Biol. 2013; 14:529–541. [PubMed: 23839576]
3. Wang ZV, Li DL, Hill JA. Heart Failure and Loss of Metabolic Control. J Cardiovasc Pharm. 2014; 63:302–313.
4. Delewi R, Andriessen A, Tijssen JGP, Zijlstra F, Piek JJ, Hirsch A. Impact of intracoronary cell therapy on left ventricular function in the setting of acute myocardial infarction: a meta-analysis of randomised controlled clinical trials. Heart. 2013; 99:225–232. [PubMed: 22875736]
5. Rane AA, Christman KL. Biomaterials for the treatment of myocardial infarction a 5-year update. J Am Coll Cardiol. 2011; 58:2615–2629. [PubMed: 22152947]
6. Ungerleider JL, Christman KL. Concise Review: Injectable Biomaterials for the Treatment of Myocardial Infarction and Peripheral Artery Disease: Translational Challenges and Progress. Stem Cells Transl Med. 2014; 3:1090–1099. [PubMed: 25015641]
7. Singelyn JM, DeQuach JA, Seif-Naraghi SB, Littlefield RB, Schup-Magoffin PJ, Christman KL. Naturally derived myocardial matrix as an injectable scaffold for cardiac tissue engineering. Biomaterials. 2009; 30:5409–5416. [PubMed: 19608268]
8. Singelyn JM, Sundaramurthy P, Johnson TD, et al. Catheter-deliverable hydrogel derived from decellularized ventricular extracellular matrix increases endogenous cardiomyocytes and preserves cardiac function post-myocardial infarction. J Am Coll Cardiol. 2012; 59:751–763. [PubMed: 22340268]
9. Seif-Naraghi SB, Singelyn JM, Salvatore MA, et al. Safety and efficacy of an injectable extracellular matrix hydrogel for treating myocardial infarction in pre-clinical animal studies. Sci Transl Med. 2013; 5:173ra25.
10. Jameel MN, Li Q, Mansoor A, et al. Long-term functional improvement and gene expression changes after bone marrow-derived multipotent progenitor cell transplantation in myocardial infarction. Am J Physiol Heart Circ Physiol. 2010; 298:H1348–H1356. [PubMed: 20173039]
11. Burt RK, Chen Y-h, Verda L, et al. Mitotically Inactivated Embryonic Stem Cells can be Utilized as an In Vivo Feeder Layer to Nurse Damaged Myocardium Following Acute Myocardial Infarction: A Pre-Clinical Study. Circ Res. 2012; 111:1286–1296. [PubMed: 22914647]
12. Lachtermacher S, Esporcatte BB, da Silva de Azevedo Fortes F, et al. Functional and Transcriptomic Recovery of Infarcted Mouse Myocardium Treated with Bone Marrow Mononuclear Cells. Stem Cell Rev and Rep. 2012; 8:251–261.
13. Pavo N, Zimmermann M, Pils D, et al. Long-acting beneficial effect of percutaneously intramyocardially delivered secretome of apoptotic peripheral blood cells on porcine chronic ischemic left ventricular dysfunction. Biomaterials. 2014; 35:3541–3550. [PubMed: 24439416]

14. Dean RA, Cox JH, Bellac CL, et al. Macrophage-specific metalloelastase (MMP-12) truncates and inactivates ELR+ CXC chemokines and generates CCL2-7-8, and-13 antagonists: potential role of the macrophage in terminating polymorphonuclear leukocyte influx. Blood. 2008; 112:3455–3464. [PubMed: 18660381]
15. Martinez FO, Sica A, Mantovani A, Locati M. Macrophage activation and polarization. Front Biosci. 2008; 13:453–461. [PubMed: 17981560]
16. Aurora AB, Porrello ER, Tan W, et al. Macrophages are required for neonatal heart regeneration. J Clin Invest. 2014; 124:1382–1392. [PubMed: 24569380]
17. Bischoff SC. Role of mast cells in allergic and non-allergic immune responses: comparison of human and murine data. Nat Rev Immunol. 2007; 7:93–104. [PubMed: 17259966]
18. Frangogiannis NG, Smith CW, Entman ML. The inflammatory response in myocardial infarction. Cardiovasc Res. 2002; 53:31–47. [PubMed: 11744011]
19. Somasundaram P, Ren G, Nagar H, et al. Mast cell tryptase may modulate endothelial cell phenotype in healing myocardial infarcts. J Pathol. 2005; 205:102–111. [PubMed: 15586361]
20. Tang L, Jennings T, Eaton JW. Mast Cells Mediate Acute Inflammatory Responses to Implanted Blomaterials. Proc Natl Acad Sci U S A. 1998; 95:8841–8846. [PubMed: 9671766]
21. Lee SH, Wolf PL, Escudero R, Deutsch R, Jamieson SW, Thistlethwaite PA. Early Expression of Angiogenesis Factors in Acute Myocardial Ischemia and Infarction. New Engl J Med. 2000; 342:626–633. [PubMed: 10699162]
22. Virag JI, Murry CE. Myofibroblast and Endothelial Cell Proliferation during Murine Myocardial Infarct Repair. Am J Pathol. 2003; 163:2433–2440. [PubMed: 14633615]
23. Davis GE, Bayless KJ, Davis MJ, Meininger GA. Regulation of Tissue Injury Responses by the Exposure of Matricryptic Sites within Extracellular Matrix Molecules. Am J Pathol. 2000; 156:1489–1498. [PubMed: 10793060]
24. Palojoki E, Saraste A, Eriksson A, et al. Cardiomyocyte apoptosis and ventricular remodeling after myocardial infarction in rats. Am J Physiol Heart Circ Physiol. 2001; 280:H2726–H2731. [PubMed: 11356629]
25. Neely JR, Morgan HE. Relationship Between Carbohydrate and Lipid Metabolism and the Energy Balance of Heart Muscle. Annu Rev Physiol. 1974; 36:413–459. [PubMed: 19400669]
26. Duncan, J.; Finck, B. PPAR/PGC-1 Regulation of Metabolism in Cardiac Disease. In: Patterson, C.; Willis, MS., editors. Translational Cardiology. New York, NY: Humana Press; 2012. p. 83-111.
27. Rowe GC, Jiang A, Arany Z. PGC-1 Coactivators in Cardiac Development and Disease. Circ Res. 2010; 107:825–838. [PubMed: 20884884]
28. Jin H, Yang R, Awad TA, et al. Effects of early angiotensin-converting enzyme inhibition on cardiac gene expression after acute myocardial infarction. Circulation. 2001; 103:736–742. [PubMed: 11156887]
29. Marín-García, J. Signaling in the Heart. New York, NY: Springer US; 2011. Signaling Pathways in Cardiovascular Development; p. 155-196.
30. Akhmedov AT, Marín-García J. Myocardial regeneration of the failing heart. Heart Fail Rev. 2012; 18:815–833. [PubMed: 23001638]
31. Oka T, Maillet M, Watt AJ, et al. Cardiac-Specific Deletion of Gata4 Reveals Its Requirement for Hypertrophy, Compensation, and Myocyte Viability. Circ Res. 2006; 98:837–845. [PubMed: 16514068]
32. Shen T, Aneas I, Sakabe N, et al. Tbx20 regulates a genetic program essential to adult mouse cardiomyocyte function. J Clin Invest. 2011; 121:4640–4654. [PubMed: 22080862]
33. Toko H, Zhu W, Takimoto E, et al. Csx/Nkx2-5 Is Required for Homeostasis and Survival of Cardiac Myocytes in the Adult Heart. Journal of Biological Chemistry. 2002; 277:24735–24743. [PubMed: 11889119]
34. Huang J, Min Lu M, Cheng L, et al. Myocardin is required for cardiomyocyte survival and maintenance of heart function. PNAS. 2009; 106:18734–18739. [PubMed: 19850880]
35. Kim Y, Phan D, van Rooij E, et al. The MEF2D transcription factor mediates stress-dependent cardiac remodeling in mice. J Clin Invest. 2008; 118:124–132. [PubMed: 18079970]

36. Azakie A, Fineman JR, He Y. Myocardial transcription factors are modulated during pathologic cardiac hypertrophy in vivo. J Thorac Cardiovasc Surg. 2006; 132:1262.e4–1271.e4. [PubMed: 17140938]

37. Furtado MB, Costa MW, Adi Pranoto EM, et al. Cardiogenic Genes Expressed in Cardiac Fibroblasts Contribute to Heart Development and Repair. Circ Res. 2014; 114:1422–1434. [PubMed: 24650916]

38. French KM, Boopathy AV, DeQuach JA, et al. A naturally derived cardiac extracellular matrix enhances cardiac progenitor cell behavior in vitro. Acta Biomater. 2012; 8:4357–4364. [PubMed: 22842035]

39. Aminzadeh MA, Tseliou E, Sun B, et al. Therapeutic efficacy of cardiosphere-derived cells in a transgenic mouse model of non-ischaemic dilated cardiomyopathy. Eur Heart J. 2015; 36:751–762. [PubMed: 24866210]

40. Ellison Georgina M, Vicinanza C, Smith Andrew J, et al. Adult c-kitpos Cardiac Stem Cells Are Necessary and Sufficient for Functional Cardiac Regeneration and Repair. Cell. 2013; 154:827–842. [PubMed: 23953114]

41. van Berlo JH, Kanisicak O, Maillet M, et al. c-kit+ cells minimally contribute cardiomyocytes to the heart. Nature. 2014; 509:337–341. [PubMed: 24805242]

42. Laurencin CT, Khan Y. Regenerative Engineering. Sci Transl Med. 2012; 4:160ed9.

Perspectives

COMPETENCY IN MEDICAL KNOWLEDGE

In animal models, injection of a hydrogel derived from decellularized porcine ventricular myocardium attenuated the decline in cardiac function following MI.

TRANSLATIONAL OUTLOOK

Clinical trials are needed to evaluate the safety and efficacy of injectable hydrogels prepared from extracellular myocardial matrix in patients with acute MI.

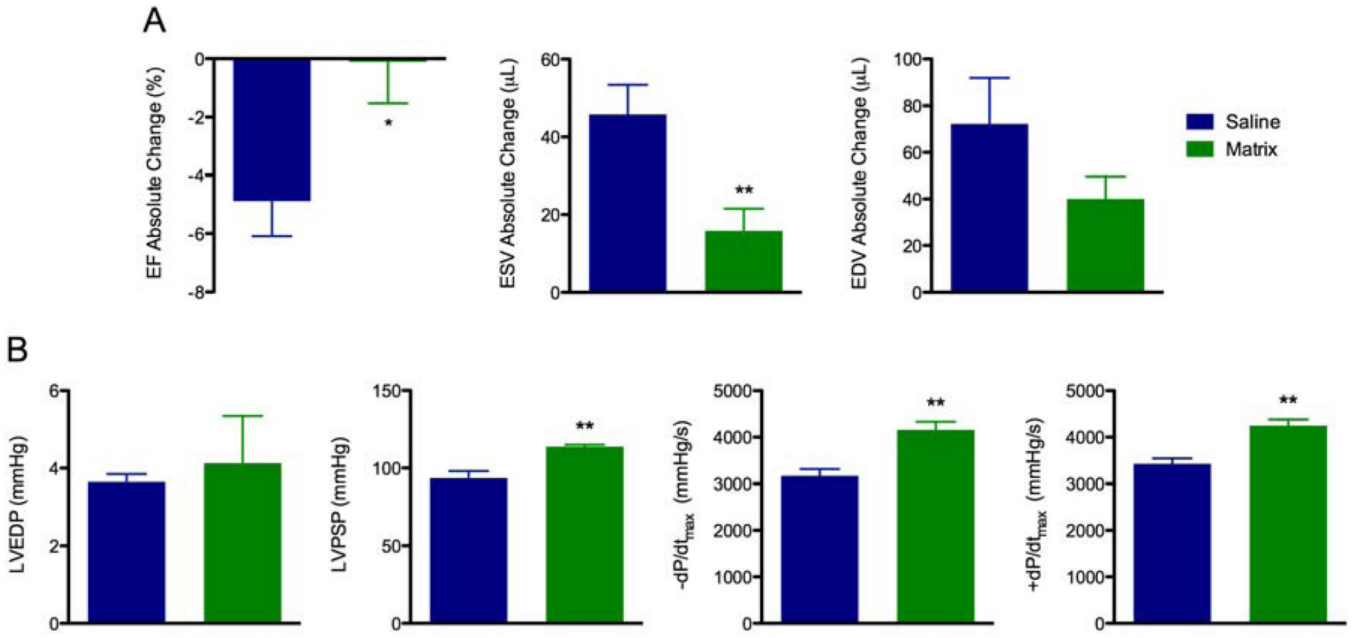

FIGURE 1. CMR and Hemodynamics Analysis

(A) Cardiac magnetic resonance imaging (CMR) was performed to compare percent changes in ejection fraction (EF), end-systolic volume (ESV), and end-diastolic volume (EDV) from 6 days post-myocardial infarction (MI) (1 day prior to injection) to 6 weeks post-MI (5 weeks postinjection) at study termination. **(B)** Left ventricular end-diastolic pressure (LVEDP), LV peak systolic pressure (LVPSP), myocardial relaxation ($-dP/dt_{max}$), and myocardial contractility ($+dP/dt_{max}$) were assessed by catheterization prior to euthanasia. *$p < 0.05$; **$p < 0.01$.

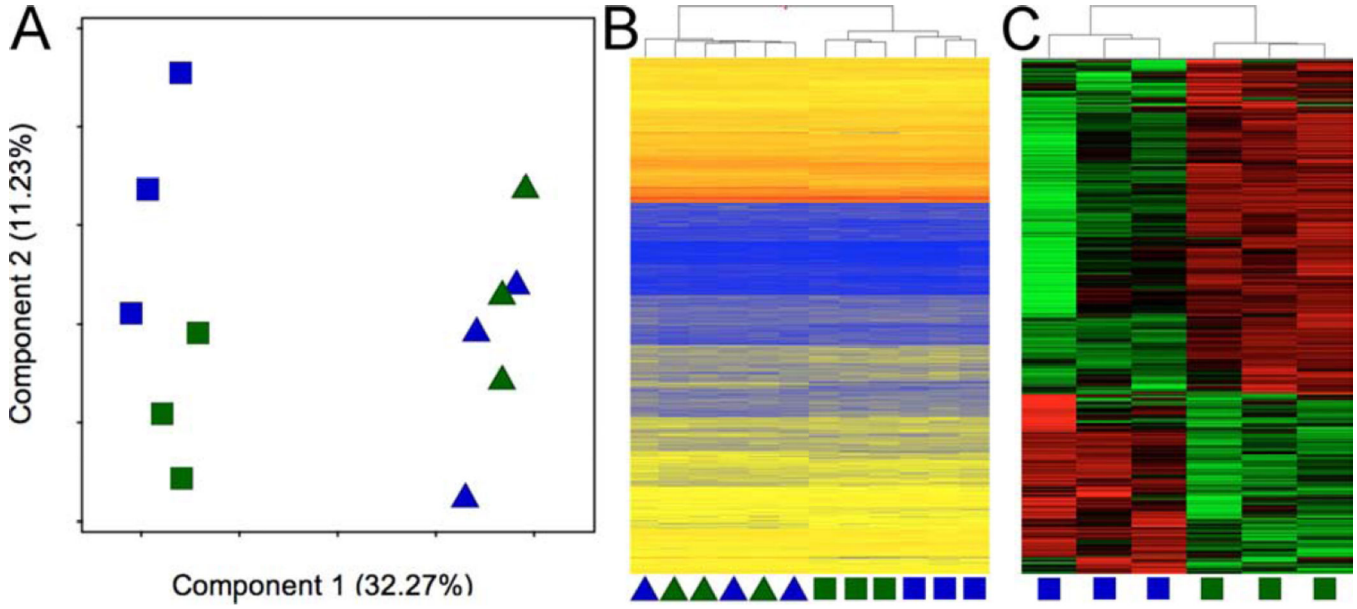

FIGURE 2. Transcriptomes Cluster Separately at 1 Week Post-injection

Principal component analysis **(A)** and hierarchical clustering **(B)** of infarct transcriptomes of all samples indicated that global gene expression after myocardial matrix injection is distinct from control saline injection by 1 week. **(C)** Hierarchical clustering of the 2,144 genes differentially expressed at 1 week post-injection. RNA from 2 infarcts were combined for analysis on 1 microarray chip to reduce biological variability (n = 3 arrays per group, per time point). Blue = saline; green = matrix; triangles = 3 days; squares = 1 week.

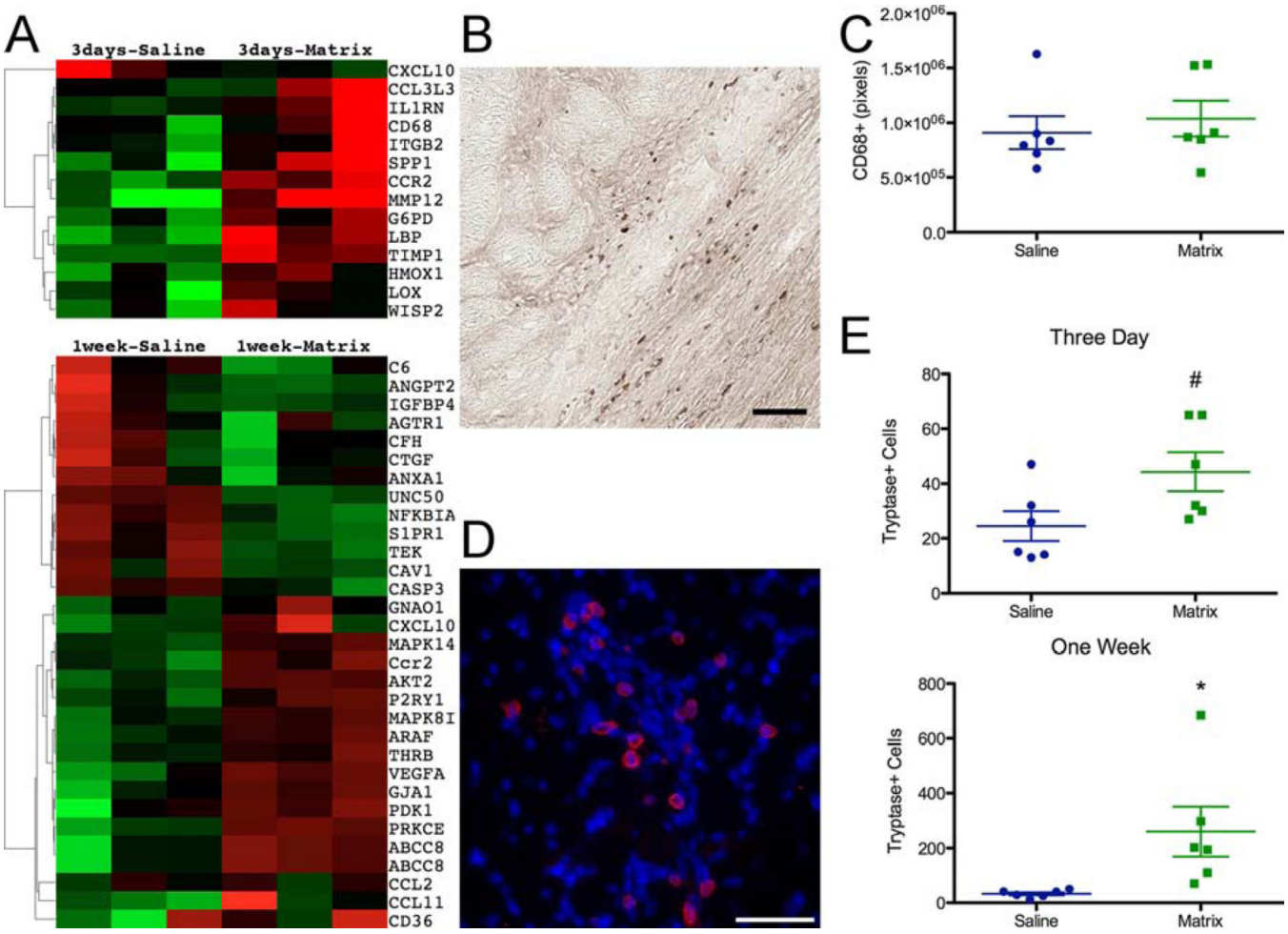

FIGURE 3. Inflammatory Response

(A) Expression of genes (red = upregulated; green =downregulated) involved in inflammation at 3 days and 1 week. **(B)** CD68+ staining for macrophages, visualized by 3,3' diaminobenzidine (brown) in a myocardial matrix-injected infarct 3 days post-injection. **(C)** Quantification of CD68 staining in the infarct wall from 3 slides at 3 days post-injection. **(D)** Tryptase+ (red) cells in myocardial matrix injected heart at 1 week post-injection; nuclei are stained blue with Hoescht 33342. **(E)** Quantification of all tryptase+ mast cells in the infarct wall from 3 slides at 3 days and 1 week post-injection. Scale bar = 50 μm; #p = 0.052, *p < 0.05.

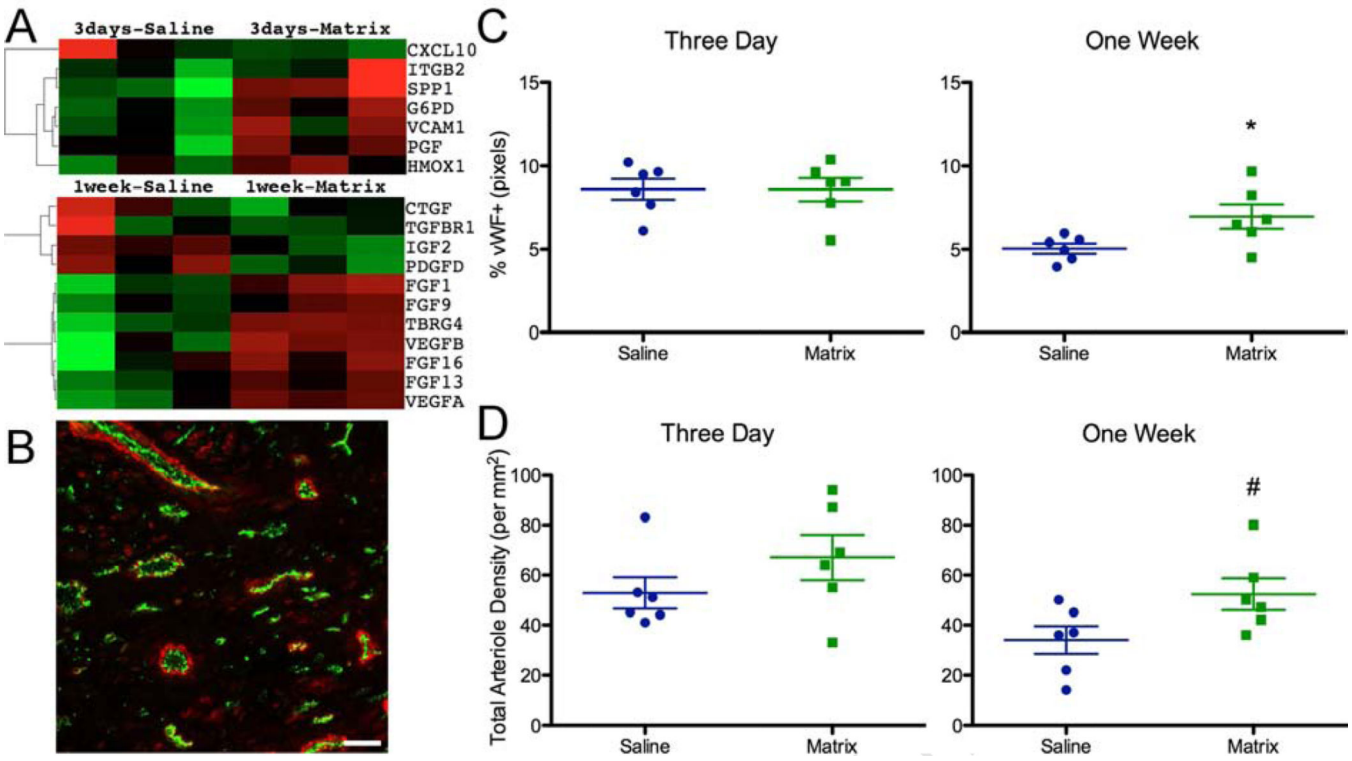

FIGURE 4. Blood Vessel Formation

(A) Expression of vessel development genes at 3 days, and growth factors at 1 week. **(B)** Representative images of vessel staining with endothelial cells labeled by von Willebrand Factor (vWF; green) and smooth muscle cells labeled with α-smooth muscle actin (red). Endothelial cells **(C)** and arteriole density **(D)** are quantified within the infarct. Scale bar = 50 μm; #$p < 0.1$; *$p < 0.05$.

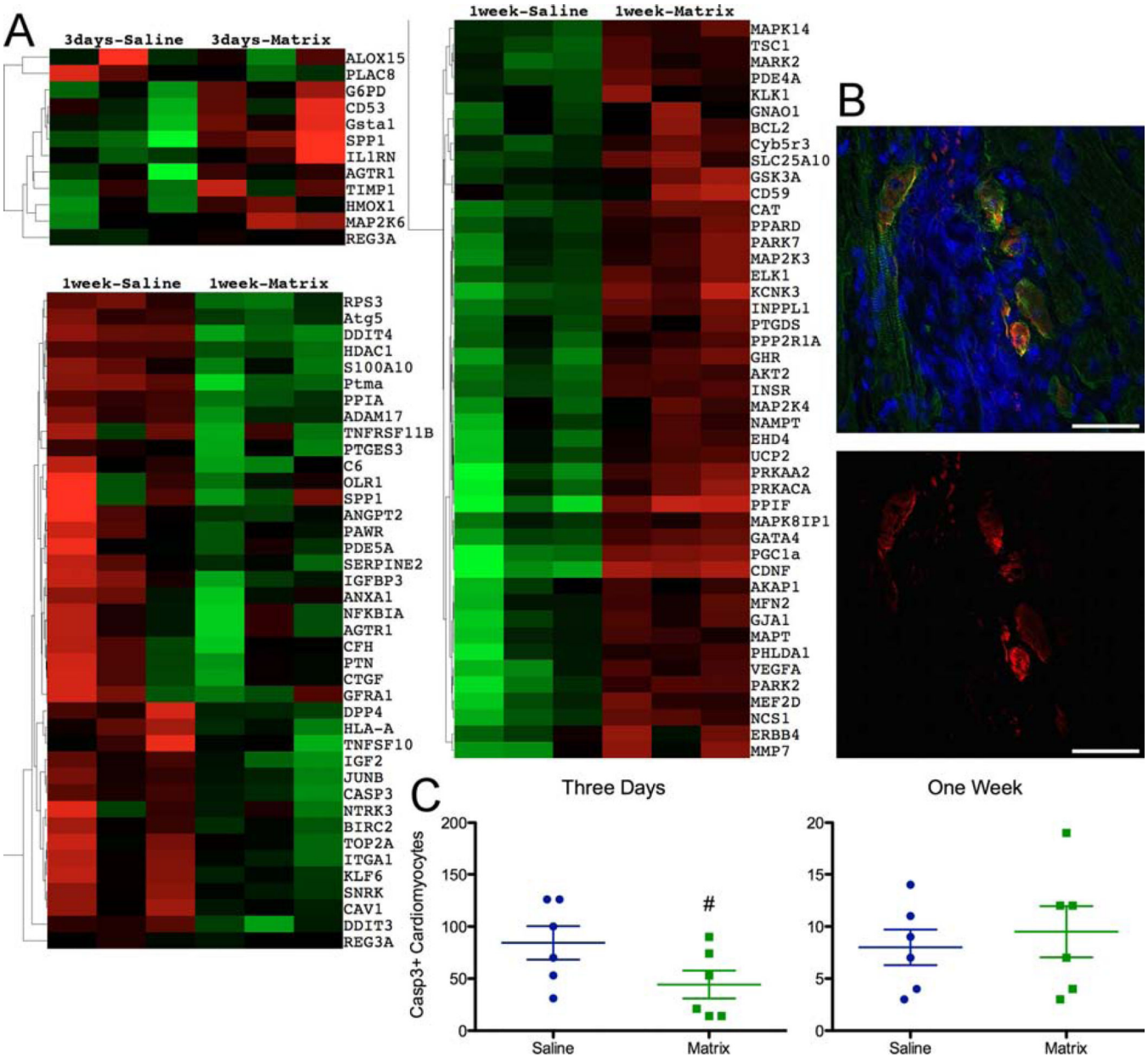

FIGURE 5. Apoptosis

(A) Expression of genes involved in apoptosis at 3 days and 1 week. **(B)** Examples of positive cleaved-Caspase3-expression (red) in α-actinin+ cardiomyocytes (green); nuclei are stained blue with Hoescht 33342 (merged image **[top]** and red-channel only **[bottom]**). **(C)** Quantification of all cleaved-Caspase3 expressing cardiomyocytes within the border zone of 3 slides. Scale bar = 50 μm; #p = 0.085.

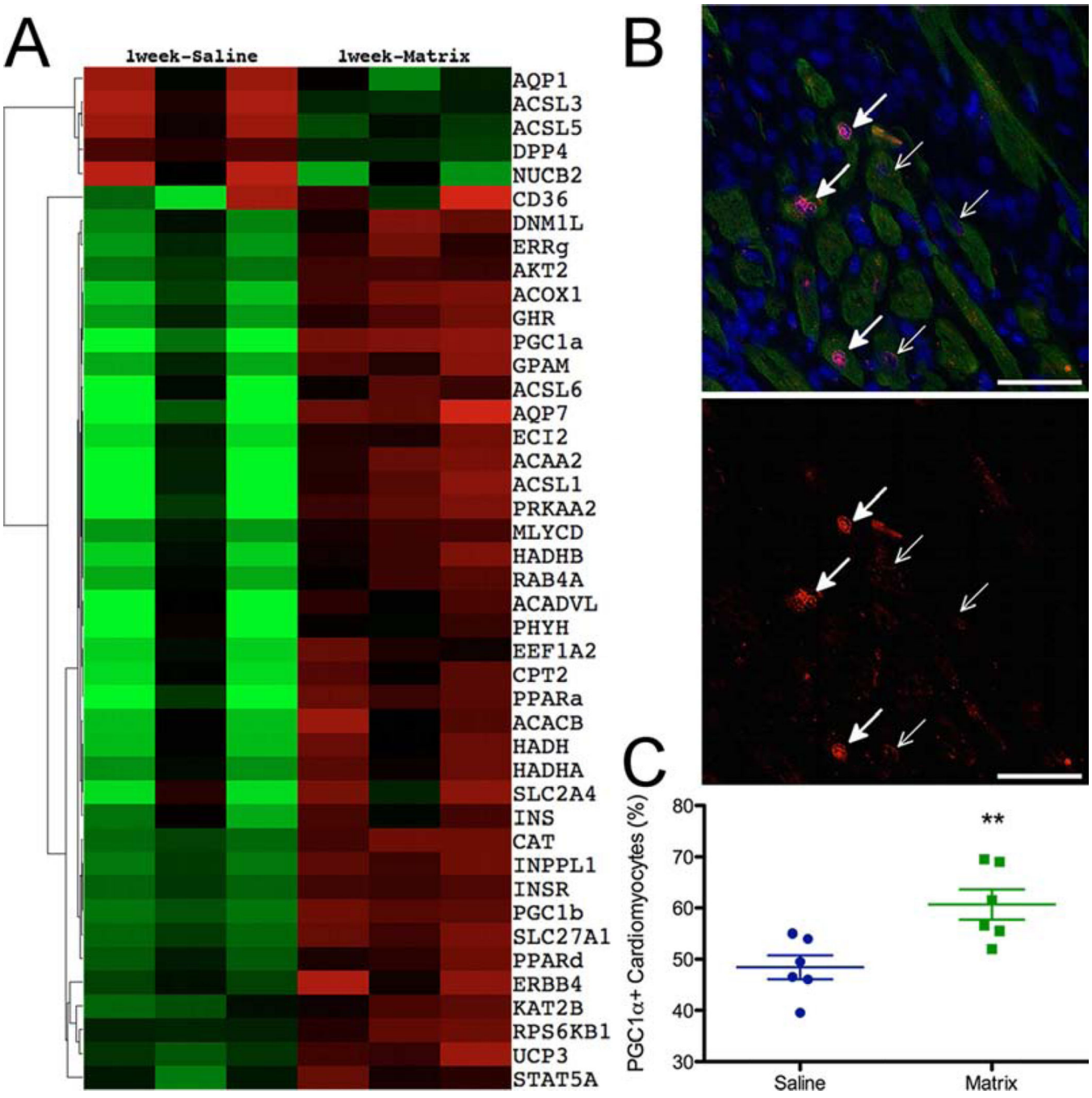

FIGURE 6. Myocardial Metabolic Gene Expression

(A) Expression of metabolic genes at 1 week. **(B)** Example of peroxisome proliferator-activated receptor gamma coactivator 1-alpha (PGC-1α) expression (red) in α-actinin+ cardiomyocytes (green) adjacent to the infarct; nuclei are stained blue with Hoescht 33342 (merged image **[top]** and red-channel only **[bottom]**). Thick arrows point to positive PGC-1α stained cardiomyocyte nuclei and thin arrows point to negative nuclei. **(C)** Quantification of PGC-1 α + nuclei expression percentage. > 200 cardiomyocytes were quantified per heart. Scale bar = 50 μm; **p < 0.01.

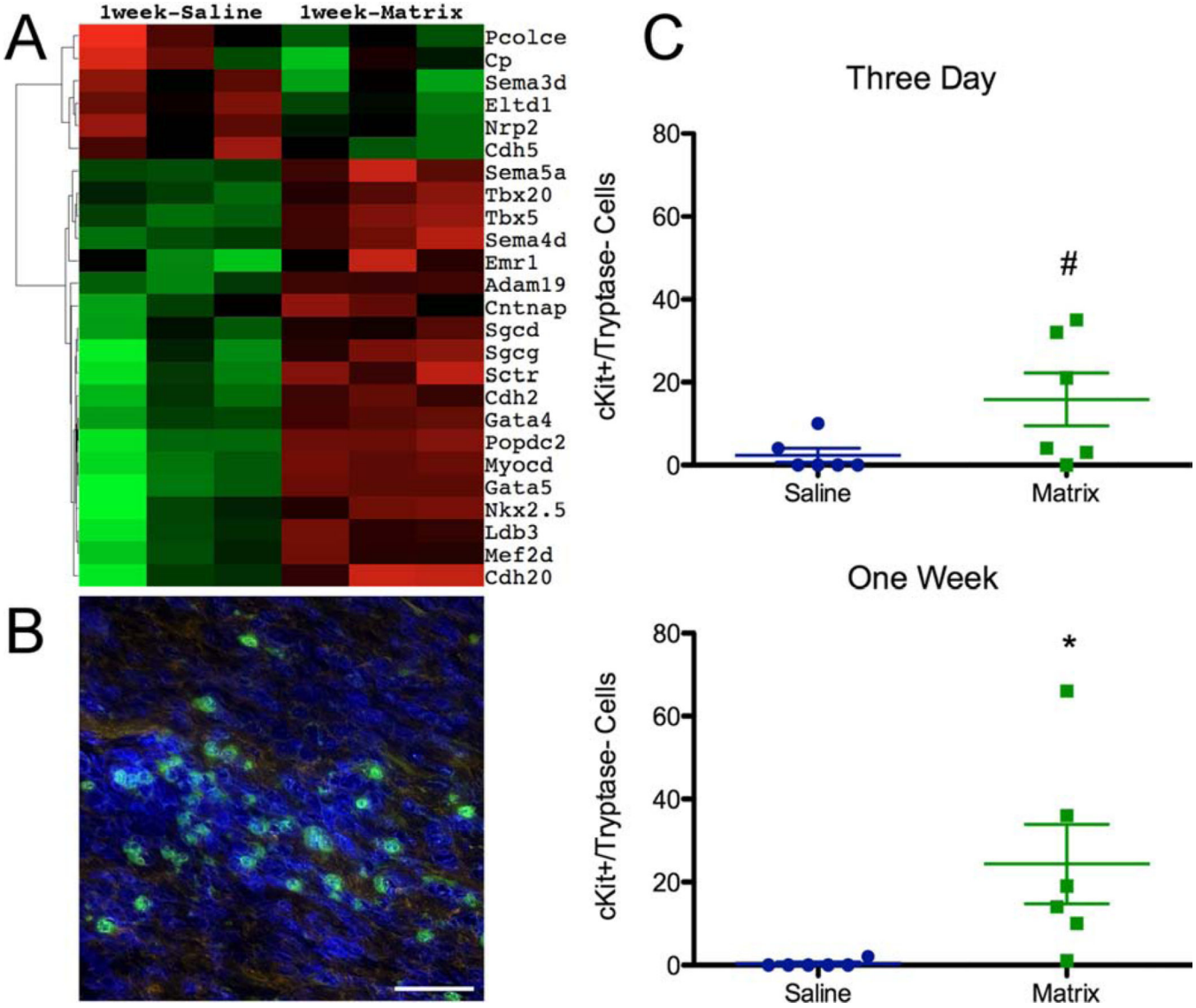

FIGURE 7. Cardiac Development

(A) Expression of genes involved in heart development. **(B)** Example of cKit+(green)/ tryptase-(red) cells with Hoescht-labeled nuclei (blue) in the myocardial matrix-injected infarct after 1 week. **(C)** Quantification of cKit+/tryptase-cells throughout border zone of 3 slides at 3 days and 1 week post-injection. Scale bar = 50 μm; #p = 0.067, *p < 0.05.

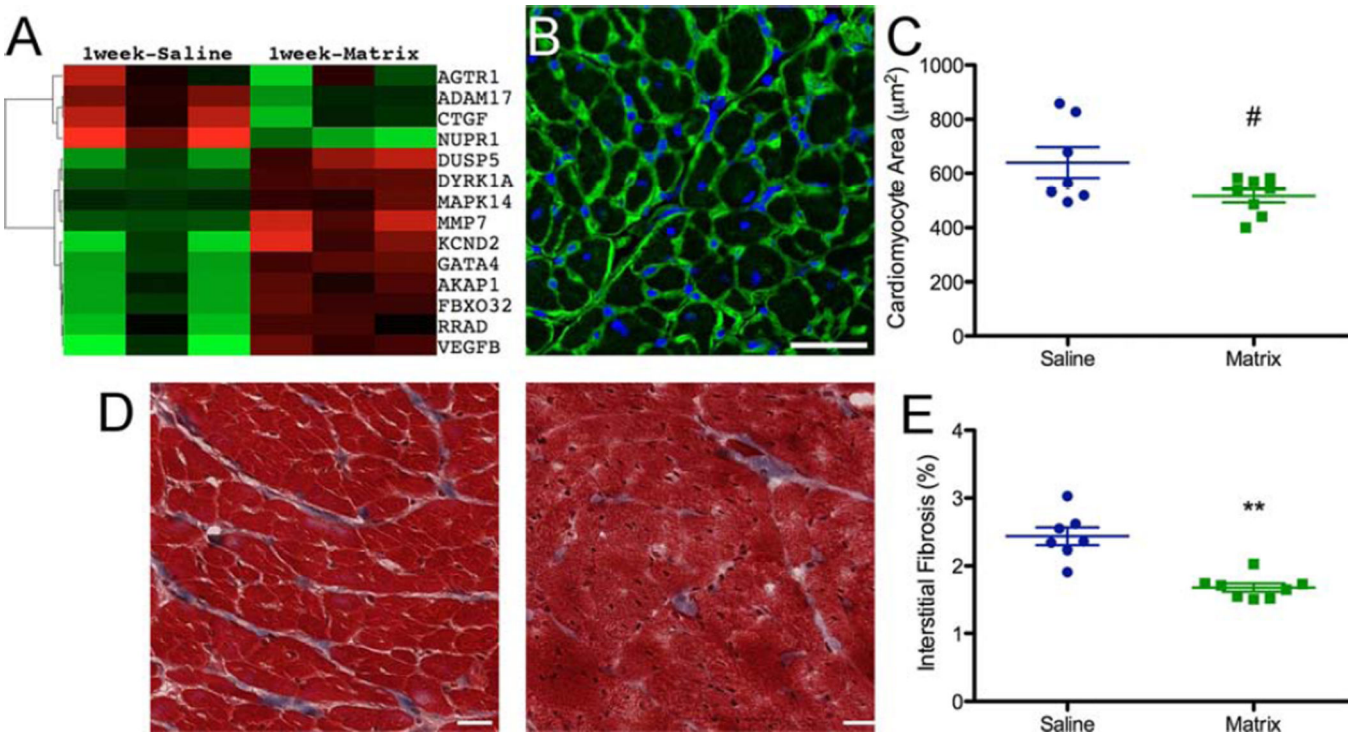

FIGURE 8. Hypertrophic Remodeling

(A) Expression of genes involved in hypertrophic response. **(B)** Representative image of the remote myocardium stained with laminin antibody (green) to outline cardiomyocytes and Hoescht 33342 to visualize nuclei (blue). **(C)** Quantification of cardiomyocyte cross-sectional area, averaged ≥300 cells per heart. **(D)** Representative Masson's Trichrome staining of interstitial fibrosis (left = saline; right = matrix). **(E)** Quantification of interstitial fibrosis from 5 slides per heart. Scale bar = 50 μm; #p = 0.061; **p < 0.01.

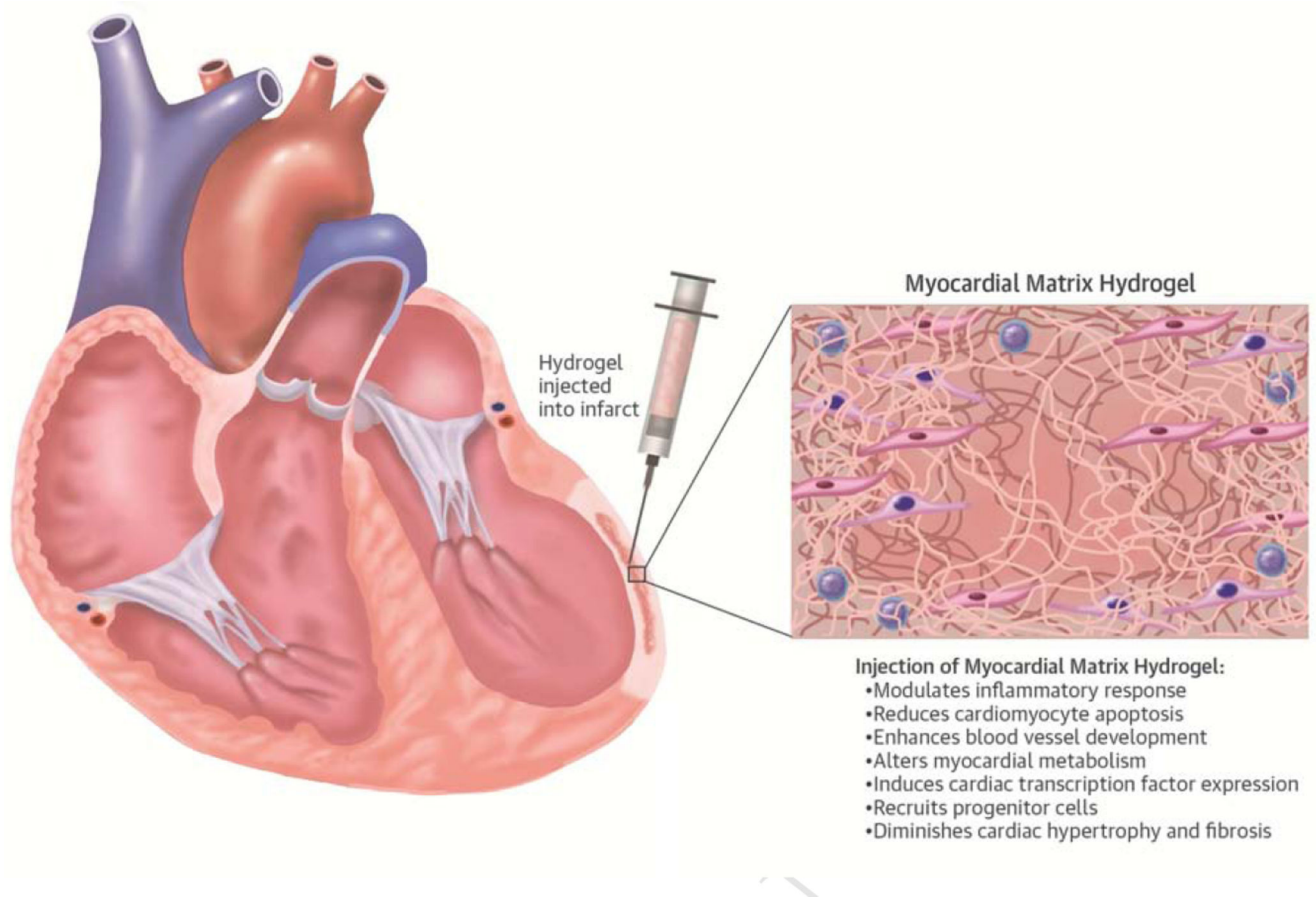

CENTRAL ILLUSTRATION. Effects of Myocardial Matrix Hydrogel Post-MI: Mechanisms Underlying the Functional Benefits

Injection of myocardial matrix 1 week post-myocardial infarction (MI) into the infarcted area induced various tissue level changes that reduced negative left ventricular remodeling and improved hemodynamics. Altering these key pathways created a pro-regenerative environment, potentially preventing or slowing development of heart failure.